

Critical exponents of Cr-containing Co-rich metallic glasses

A. Das and A. K. Majumdar

Department of Physics, Indian Institute of Technology, Kanpur 208016, Uttar Pradesh, India

(Received 10 January 1992; revised manuscript received 12 June 1992)

The critical exponents of the ferromagnetic-to-paramagnetic transition of amorphous $\text{Fe}_5\text{Co}_{50}\text{Ni}_{17-x}\text{Cr}_x\text{B}_{16}\text{Si}_{12}$ ($x=5, 10, \text{ and } 15$) alloys have been studied by low-field ac-susceptibility and dc-magnetization measurements. The values of β_{eff} , γ_{eff} , and δ for the alloys with $x=5$ and 10 , in the asymptotic critical region, agree with those of other amorphous materials and are closer to the predictions of the three-dimensional Heisenberg model. In contrast, for the sample with $x=15$, the effective values of the exponents β (0.52) and γ (1.73) are significantly larger. This difference is ascribed to the formation of magnetic clusters with the addition of Cr, which leads to the nondivergence of the correlation function at T_c and consequently a different set of exponent values. Further, these results strengthen the conclusion that there is no influence of topological disorder on the values of the exponents in the critical region.

I. INTRODUCTION

The nature of phase transitions in disordered materials has been an area of study that has attracted considerable interest both on theoretical and experimental fronts.¹ Theoretical understanding is divided on the issue of the role of disorder. Fisher² has shown that, in systems with annealed disorder, the critical indices are not influenced by the disorder if the specific-heat exponent $\alpha < 0$. Based on phenomenological arguments, Harris³ has put forward a criterion: if the specific heat exponent α is negative for an ordered system, the critical exponents would remain unchanged in the presence of weak, spatially random disorder. Renormalization-group theory-based calculations^{4,5} also arrive at the same conclusion. There are, however, other theoretical calculations⁶ that contradict the above conclusion and suggest that the critical indices of the system with $\alpha < 0$ will depend on the amount of quenched disorder present. A new set of fixed points is suggested when the systems are close to the critical concentration x_c for the appearance of long-range ferromagnetic order. In the limit $x \rightarrow x_c$, the numerical values of the indices are $\alpha = -1$, $\beta = 0.5$, $\gamma = 2.0$, and $\delta = 5$ for the exponents of specific heat, magnetization, susceptibility, and isothermal magnetization, respectively.

It has been shown⁷ by careful experimentation and data analysis that the value of the exponent γ agrees exactly with the theoretically predicted value for the 3D Heisenberg system⁸ in the asymptotic critical regime (ACR), if proper corrections are made to the experimentally measured value of γ . The correction parameters have their origin in the higher-order derivatives of the Gibb's potential. A survey of experimental results supports the view that the phase transition in amorphous materials is not influenced by the topological disorder and behaves in the same manner as homogeneous crystalline systems. The influence of disorder is mainly at temperatures beyond the true critical region, i.e., in the intermediate region between the mean field and the ACR,

where $\gamma(T)$ describes a nonmonotonic behavior (for a review see Ref. 9).

Experimental results of amorphous systems containing Cr or Mn, around the critical concentration x_c , however, are different.¹⁰ It is found that as $x \rightarrow x_c$ in these alloys, $\beta \rightarrow 0.5$, $\gamma \rightarrow 2$, and $\delta \rightarrow 5$. Specific-heat measurements¹¹ near the T_c of Cr-containing glasses indicate a smeared transition with negligible peak height. The temperature derivative of the resistivity also shows a broad transition region. These results point to the formation of magnetic clusters with distribution of T_c 's which result in the deviation of critical exponents from those of the homogeneous systems.

Here we report results on a set of Fe-Co-Ni-Cr-B-Si alloys where Ni is being continuously replaced by Cr. The concentration is such that it is sufficiently away from the critical concentration. It exhibits a ferromagnetic behavior below T_c down to the lowest temperature of ≈ 20 K without an indication of any transition to another phase. These samples show a broad resistivity minimum at temperatures around 200 K, and have no discernible discontinuity in the resistivity at their respective T_c 's.¹² Magnetic fields as high as 16 kOe produce no change in the behavior below the minimum. Also, the magnetoresistance results are not identifiable with the standard results of conventional ferromagnets.¹³ But the magnetization data seem to support spin-wave behavior at temperatures below $0.5T_c$. These results put together make this alloy system an interesting choice for study near its phase transitions. The motivation behind the present work is to see if the same set of critical indices, as found in other ferromagnets, describes its phase transition.

II. EXPERIMENT

The magnetic measurements were done on the melt-quenched amorphous ribbons (typical width 1 mm, thickness 0.027 mm) of nominal composition $\text{Fe}_5\text{Co}_{50}\text{Ni}_{17-x}\text{Cr}_x\text{B}_{16}\text{Si}_{12}$ ($x=5, 10, \text{ and } 15$, designated

as $A2$, $A3$, $A4$, respectively). X-ray measurements confirmed the amorphous nature of the samples. For χ_{ac} measurements, four pieces of the above-mentioned ribbons, 4 cm in length were used. The primary and the two secondary coils were kept immersed in a liquid-nitrogen bath. The coils were connected to a locally fabricated mutual inductance bridge and the off balance signal ($\propto \chi$) was measured with a lock-in amplifier (PAR 5208). The bridge was operated at a frequency of 313 Hz and the ac field was 0.3 Oe. A copper-Constantan thermocouple was used to sense the temperature. Data points were taken at intervals of 30 mK.

dc-magnetization measurements were made by a vibrating sample magnetometer (PAR 155) in conjunction with a closed-cycle helium refrigerator (RMS, Cryosystems). A 100- Ω platinum resistance thermometer was used to measure the temperature. Magnetic moments, every 1 K apart at several constant dc magnetic fields (up to 16 kOe), were measured in the range $T_c \pm 30$ K.

III. RESULTS AND DISCUSSION

A. Analysis

The critical exponents describing the ferromagnetic-to-paramagnetic transition are obtained from the following relations:

$$M = B(T - T_c)^\beta, \text{ for } T < T_c, \quad (1)$$

$$\chi = \Gamma(T - T_c)^{-\gamma}, \text{ for } T > T_c, \quad (2)$$

and

$$M = DH^{1/\delta} \text{ at } T = T_c, \quad (3)$$

where B , Γ , and D are the critical amplitudes. The three exponents are related by the scaling relation¹⁴

$$\beta\delta = \beta + \gamma. \quad (4)$$

There are several methods of obtaining the exponents from the above relations.¹ Our method of analysis is as follows: from the low-field χ_{ac} measurements we obtain χ as a function of T for $T > T_c$. From the demagnetization corrected value of χ (the demagnetization factor $\simeq 0.01$), γ is obtained from the Kouvel-Fisher plot.¹⁵ In this, relation (2) is expressed as

$$X(T) = \chi^{-1} \left[\frac{d}{dT} \chi^{-1} \right]^{-1} = \frac{1}{\gamma_{\text{eff}}} (T - T_c). \quad (5)$$

The slope and intercept of the plot of the function $X(T)$ provide γ_{eff} and T_c , respectively. This method has the advantage that a prior knowledge of T_c is not essential. A three-point derivative of χ^{-1} is taken, thus smoothing the data over a small region ($\simeq 100$ mK). The values of γ_{eff} and T_c with the uncertainties are obtained using a least-squares-fit program and are given in Table I. The results of this analysis are plotted in Fig. 1, which shows X as a function of $\epsilon = (T - T_c)/T_c$, for samples $A2$ and $A3$. In this figure the data for sample $A2$ are displaced along the vertical axis and therefore they do not pass through the origin. However, the data for $A3$ are not displaced and hence they pass through the origin. A sample of Metglas 2826A (Allied Chemicals) was also measured to verify the results as the values of γ and T_c exist in the literature.¹⁶ We obtain for sample 2826A, $\gamma = 1.35$ and $T_c = 225.3$ K where the range of analysis is confined to $\epsilon = (3.15 - 47.5) \times 10^{-3}$. The values are in good agreement with those reported. The T_c obtained by the KF method matches that obtained by the derivative method, except for sample $A4$. In $A4$, the T_c differs by about 7 K between these two methods.

From dc-magnetization measurements the values of β , γ , and δ are obtained. A plot of $\ln M$ vs $\ln H$ is made at T_c . Figure 2 shows the plots for samples $A2$ and $A3$. The values of δ are estimated from the slopes of these straight lines. For sample $A4$, the slope near T_c was strongly temperature dependent. In the absence of $M(H)$

TABLE I. Values of β_{eff} , γ_{eff} , δ , and T_c of $A2$, $A3$, and $A4$. VSM: vibrating sample magnetometer; ACS: ac susceptibility. The numbers in brackets indicate the uncertainty in the least significant figure and are obtained from the confidence limits of the best-fitted parameters of the least-squares fit.

	Method	$A2$	$A3$	$A4$	Heisenberg 3D (Ref. 8)
T_c (K)	ACS	267.0(1)	222.3(3)		
	VSM	268.1(8)	222.5(7)	174.0(8)	
α^a		0.2	-0.2	-0.7	
β_{eff}	VSM	0.35(1)	0.41(1)	0.52(3)	0.365
γ_{eff}	ACS	1.19(1)	1.38(2)		1.387
(Range of fit)	$\epsilon \times 10^3$	2.2-25	3.1-32		
γ_{eff}	VSM	1.19(2)	1.30(3)	1.73(6) ^b	
δ	VSM	4.42(1)	4.49(5)	4.32(14)	4.803
B		38.7	44.7	57.7	
Γ^{-1}		10 000	11 600	15 800	
$M(0)$ (emu/g)		48.1	44.7	40.8	
$\bar{\mu}$ (μ_B /at.)		0.42	0.38	0.34	

^aCalculated from Rushbrook inequality $\alpha = 2(1 - \beta) - \gamma$.

^bObtained from scaling analysis; $\epsilon = (T - T_c)/T_c$.

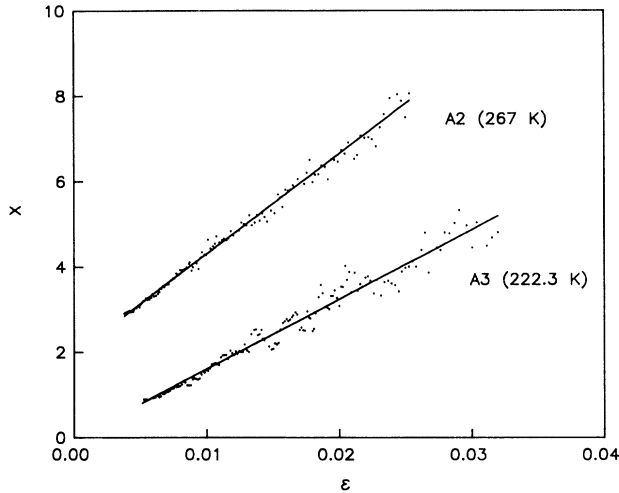


FIG. 1. Plot of $X [= \chi^{-1}(d\chi^{-1}/dT)^{-1}]$ vs $\epsilon(T-T_c/T_c)$ of $A2$ and $A3$ ($\text{Fe}_5\text{Co}_{50}\text{Ni}_{17-x}\text{Cr}_x\text{B}_{16}\text{Si}_{12}$, $x=5$ and 10 , respectively). The figures in parentheses indicate the respective T_c 's. The data of $A2$ are displaced along the vertical axis. The continuous lines are obtained from least-squares analysis.

data exactly at $T_c = 174$ K, δ was plotted as a function of temperature over an interval of 8 K around T_c , from which the value of δ at 174 K was obtained. The values of δ for the three samples are given in Table I. We find that δ of sample $A4$ (≈ 4.3) is slightly lower than those of $A2$ and $A3$ (≈ 4.45) and also the error in it is relatively large, which may partly be due to the extrapolation procedure adopted. To estimate M_S we consider the Arrott-Noakes equation of state,¹⁷

$$\left[\frac{H}{M}\right]^{1/\gamma} = \left[\frac{T-T_c}{T_1}\right] + \left[\frac{M}{M_1}\right]^{1/\beta}, \quad (6)$$

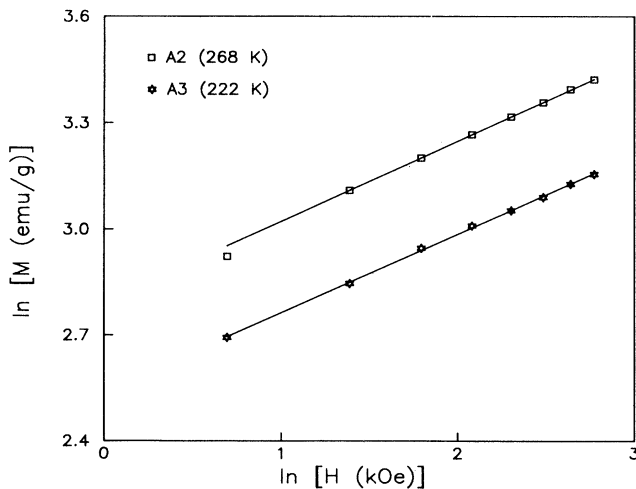


FIG. 2. $\ln M$ vs $\ln H$ plot near the T_c of $A2$ and $A3$ ($\text{Fe}_5\text{Co}_{50}\text{Ni}_{17-x}\text{Cr}_x\text{B}_{16}\text{Si}_{12}$, $x=5$ and 10 , respectively) for determining δ .

with the material parameters M_1 and T_1 . With proper choices of β and γ , a plot of $(M)^{1/\beta}$ vs $(H/M)^{1/\gamma}$ gives a set of straight lines near T_c . The intercepts on the $M^{1/\beta}$ and $(H/M)^{1/\gamma}$ axes give M_S and χ^{-1} , respectively. Using Eq. (4), an equivalent form of this graph (not shown) could be plotted between $M^{\delta-1}$ vs H/M . Near T_c , the data points fall on a straight line. The low-field data points deviate from the straight line. From the intercepts of the high-field data of the isotherms near T_c , extrapolated to $H=0$ (H corrected for demagnetization), we obtain M_S . The Kouvel-Fisher method of analysis allows us to obtain β and T_c by rewriting Eq. (1) in the form

$$Y(T) = M_S \left[\frac{d}{dT} M_S \right]^{-1} = \frac{1}{\beta_{\text{eff}}} (T - T_c). \quad (7)$$

The plot of $Y(T)$ vs T is a straight line whose intercept and slope give T_c and β , respectively. But here, Y vs $-\epsilon$ is plotted in Fig. 3, where the data for samples $A3$ and $A4$ are displaced along the vertical axis and therefore do not pass through the origin (unlike $A2$). The values of β obtained are in the range $0.35-0.52$. The exponent in the range $T > T_c$ is obtained from $M^{3.5}$ vs H/M plots. The high-field intercepts on the H/M axis provide $1/\chi$ at different temperatures. Then, using the method of Kouvel and Fisher, γ and T_c are obtained. The values of γ and T_c (within 1 K) agree with those obtained from the low-field χ_{ac} measurements (Table I). The value of γ , obtained from dc magnetization measurements, however, suffers from the nonlinearity in $M^{1/\beta}$ vs $(H/M)^{1/\gamma}$ plots, particularly at low fields. Therefore, it is not uncommon to observe disagreement between the results obtained from χ_{ac} and dc magnetization measurements. The analysis has been confined to a narrow region of temperature around T_c . As we go father away from T_c , the curvature in the plots increases to such an extent that it be-

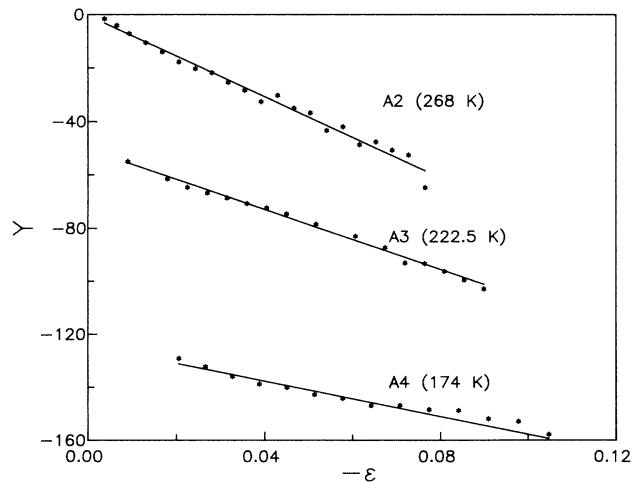


FIG. 3. Plot of $Y [= M_S(dM_S/dT)^{-1}]$ vs $-\epsilon[\epsilon=(T-T_c)/T_c]$ of $A2$, $A3$, and $A4$ ($\text{Fe}_5\text{Co}_{50}\text{Ni}_{17-x}\text{Cr}_x\text{B}_{16}\text{Si}_{12}$, $x=5$, 10 , and 15 , respectively). The figures in parentheses indicate the respective T_c 's. The data of $A3$ and $A4$ are displaced along the vertical axis.

comes difficult to make a linear extrapolation. Due to this restriction, the region beyond the asymptotic critical regime has not been analyzed.

The magnetic equation of state is a relationship among the variables M , H , and T . Using the scaling hypothesis, this can be written as

$$\frac{M(\varepsilon, H)}{|\varepsilon|^\beta} = M \left(\frac{\varepsilon}{|\varepsilon|}, \frac{H}{|\varepsilon|^{\beta\delta}} \right). \quad (8)$$

In terms of the variables $m \equiv |\varepsilon|^{-\beta} M(\varepsilon, H)$ and $h \equiv |\varepsilon|^{-\beta\delta} H(\varepsilon, M)$, called the scaled magnetization and scaled magnetic field respectively, the above equation can be written as

$$m = f_{\pm}(h). \quad (9)$$

This relation shows that m , as a function of h , falls on two curves: one for $T < T_c$ and the other for $T > T_c$. If the scaling relations are valid and a correct choice of β , γ , and δ is made, then in a plot for $\ln m$ vs $\ln h$, all the data points collapse onto two branches [Figs. 4(a)–4(c)].

Due to the relatively higher uncertainty in all the exponent values of sample *A4* (see Table I), the plot for this sample [Fig. 4(c)] is not as satisfactory as those of *A2* and *A3* [Figs. 4(a)–4(b)]. For a large value of $\ln h$, the data may be fitted to a straight line, the slope of which is $1/\delta$. It is still better to plot m^2 vs h/m to verify the scaling relations.¹ Figures 5(a)–5(c) show this plot for *A2*, *A3*, and *A4*; data points only above $H_{\text{ext}} = 2$ kOe have been shown in the figure. It also shows that the scaling equations are valid over a wide region of temperature both above and below T_c . The intercepts on the axes give m_0^2 and h_0/m_0 . These are related to the critical amplitudes B and Γ in the following manner:

$$B = m_0, \quad T < T_c,$$

and

$$\Gamma^{-1} = (h_0/m_0), \quad T > T_c. \quad (10)$$

These values are included in Table I. h_0 is identified with the effective exchange interaction field.

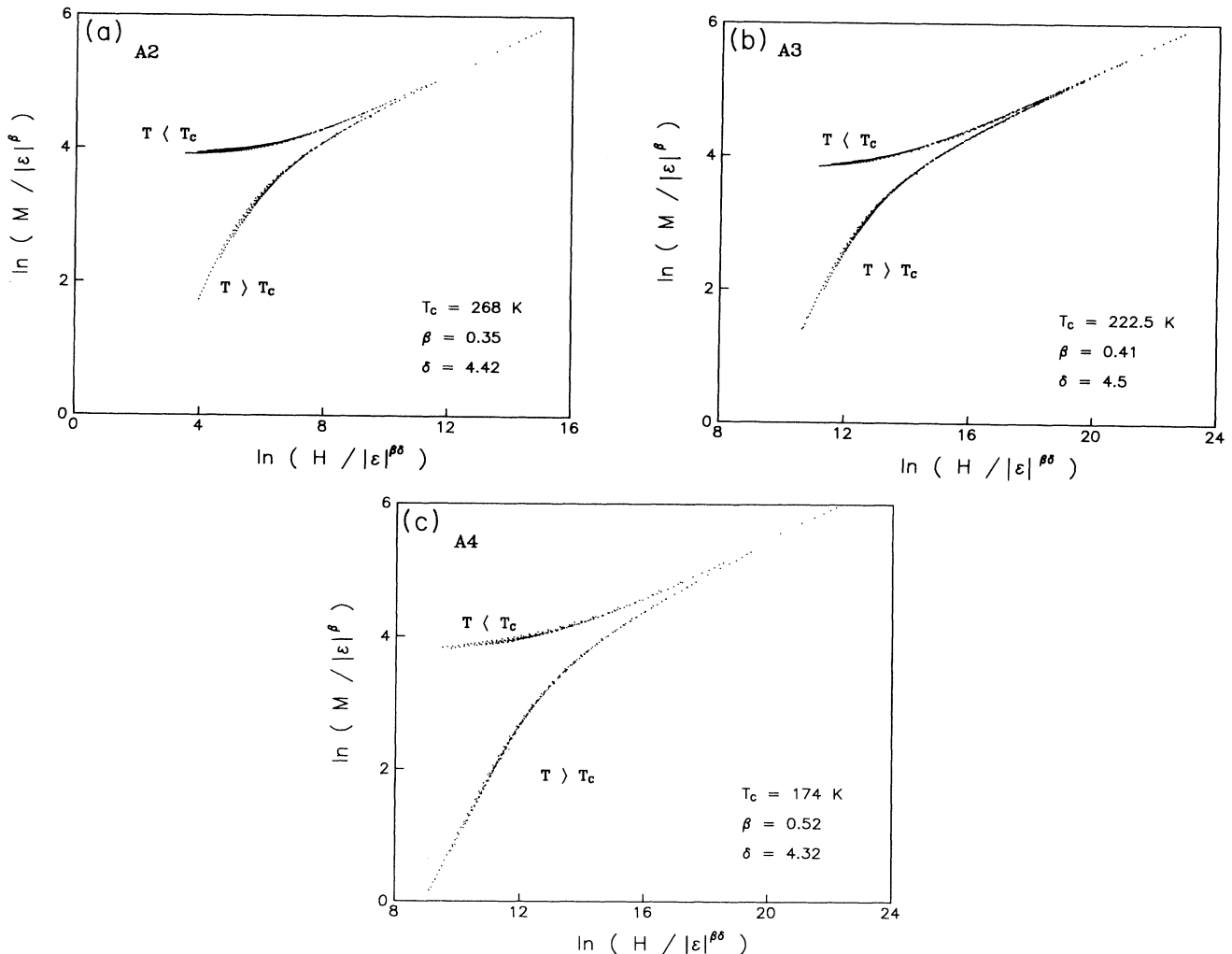


FIG. 4. (a)–(c) Scaling plot for *A2*, *A3*, and *A4* ($\text{Fe}_5\text{Co}_{50}\text{Ni}_{17-x}\text{Cr}_x\text{B}_{16}\text{Si}_{12}$, $x = 5, 10$, and 15 , respectively).

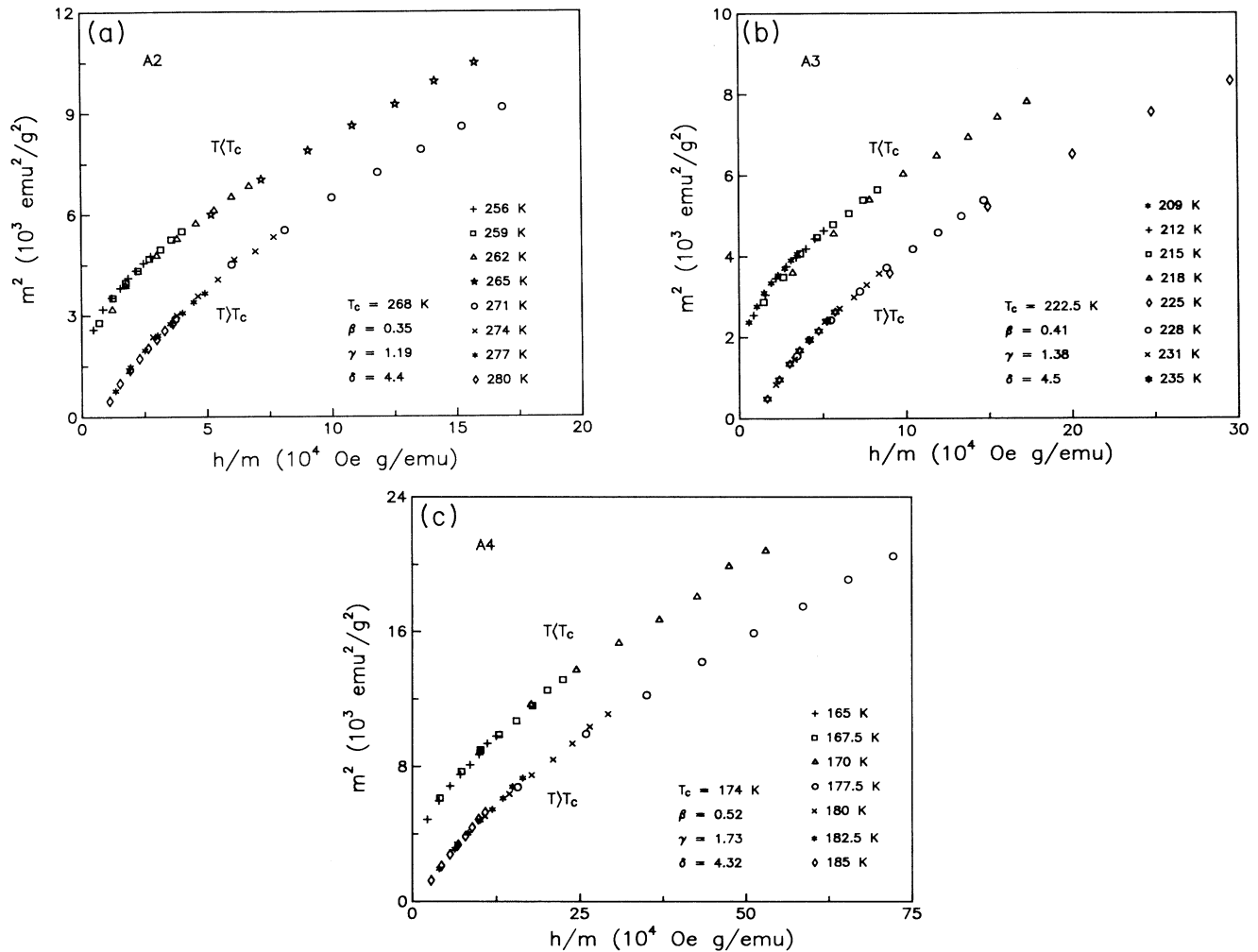


FIG. 5. (a)–(c) Plot of m^2 vs h/m for $A2$, $A3$, and $A4$ ($\text{Fe}_5\text{Co}_{50}\text{Ni}_{17-x}\text{Cr}_x\text{B}_{16}\text{Si}_{12}$, $x = 5, 10$, and 15 , respectively).

B. Discussion

Table I summarizes the values of T_c , β , γ , and δ obtained for samples $A2$, $A3$, and $A4$. With the substitution of Ni by Cr, the T_c decreases monotonically by about 8 K/at. % Cr. The value of δ remains nearly the same for the three samples but is lower than the theoretical estimate of 4.8. It is found that this exponent varies in the range 2.8–6.8 for amorphous ferromagnets.¹ β exhibits a small concentration dependence, although in the case of $A2$ and $A3$, it is closer to the Heisenberg value of 0.365. The experimentally determined values are more in the vicinity of 0.40. But $A4$ has a value of β that is higher than those of $A2$ and $A3$. The value of γ is the most often experimentally determined one and is normally used as evidence for or against the various existing theories. The sample $A2$ shows an uncharacteristically low value for γ . The value (ACS) for $A3$ matches the 3D Heisenberg value. With further addition of Cr ($A4$), γ increase to 1.73. Thus, while we observe that with the addition of Cr, the coefficients β and γ increase beyond the uncertainties associated with them, the changes in the exponents are relatively small in the case of $A2$ and $A3$.

Their values are closer to the theoretically estimated ones for homogeneous systems. For sample $A4$ (large Cr) the exponents β and γ are significantly larger and different from those of $A2$ and $A3$. In all these alloys the indices obey the scaling equation of state over the whole range of temperature. Assuming that the Rushbrooke inequality holds, an estimate of the value of the specific heat exponent is made. It gives $\alpha = 0.2$, -0.2 , and -0.7 for $A2$, $A3$, and $A4$, respectively.

It is observed that there exists a significant curvature in the $M(H)$ plots for all three samples at $T > T_c$. In the case of $A4$, the curvature is seen to exist even beyond $1.4T_c$. In the case of $A2$ and $A3$, the region up to only $1.15T_c$ could be studied. The nonlinearity in the $M(H)$ curve, beyond T_c , is known to arise due to superparamagnetic clusters. In a structurally disordered material there is a tendency towards the formation of localized clusters of strongly interacting moments, giving rise to superparamagnetism.¹⁸ Another criterion for superparamagnetic behavior is that a plot of M vs H/T should give a universal curve. In our studies, although a large curvature is observed, it does not show the universal nature. Similar behavior is also observed in other Ni-rich alloys¹⁹

and is attributed to the formation of clusters that are not independent of temperature, and interact among themselves. One plausible explanation for the deviation of the indices in sample *A4* from those of a homogeneous system could be the existence of these clusters. The presence of clusters in Cr-containing samples has been inferred from specific heat,^{11,20} and neutron-diffraction measurements.²¹ It is also found that the presence of Cr smears the transition. In addition, neutron-scattering measurements on Fe-Cr and Fe-Mn based glasses²¹ show that the spin-spin correlation length ξ does not diverge at T_c . In general, the influence of disorder is not observed in the true critical region, the reason being that as $T \rightarrow T_c$, there are strong correlations in the spin system and all spins within a range described by $\xi(T)$ interact cooperatively and the effect of disorder on a length scale smaller than $\xi(T)$ is reduced.⁹ The effect of disorder is observed only at higher temperatures where $\xi(T)$ becomes small compared to atomic scale inhomogeneities. Thus, the nondivergence of $\xi(T)$ at T_c due to the presence of clusters may be responsible for the anomalous behavior of the exponents in *A4*. Alloys near $x \approx x_c$ also exhibit similar values of exponents.

IV. CONCLUSIONS

From the present measurements we are able to conclude that the presence of quenched disorder does not

lead to significant change in the exponents as is evident from the results of *A2* and *A3* where the Cr contents are relatively small. The exponents do not match *exactly* the theoretical values but are in conformity with other experimental results. This difference in the theoretically predicted and the experimentally measured values has been discussed^{1,22} and is attributed to the presence of long-range interactions in the system. We find that in samples *A2* and *A3* the exponents β and γ increase with the addition of Cr but the increase is relatively small. The exponents are closer to the theoretically estimated values for homogeneous systems. However, in *A4* the values of exponents β and γ are large and significantly different from those of *A2* and *A3* because of magnetic clustering. On the other hand, they are very similar to those observed in compositions close to the critical concentration. Recently, Houer and Wagner²³ have shown that deviations from Heisenberg values need not be limited to compositions close to the critical concentration and may be observed in materials further away from x_c .

ACKNOWLEDGMENT

Financial assistance from project No. SP/S2/M-45/89 of the Department of Science and Technology, Government of India, is gratefully acknowledged.

¹S. N. Kaul, *J. Magn. Magn. Mater.* **53**, 5 (1985).

²M. E. Fisher, *Phys. Rev.* **176**, 257 (1968).

³A. B. Harris, *J. Phys. C* **7**, 1671 (1974).

⁴G. Grinstein and A. Luther, *Phys. Rev. B* **13**, 1329 (1976).

⁵A. Weinrib and B. I. Halperin, *Phys. Rev. B* **27**, 413 (1983).

⁶G. Sobotta, *J. Magn. Magn. Mater.* **28**, 1 (1982); *Solid State Commun.* **43**, 875 (1982).

⁷S. N. Kaul, *Phys. Rev. B* **38**, 9178 (1988).

⁸J. C. Le Guillon and J. Zinn-Justin, *Phys. Rev. Lett.* **39**, 95 (1977).

⁹M. Fähnle, G. Herzer, H. Krönmüller, R. Meyer, M. Saile, and T. Egami, *J. Magn. Magn. Mater.* **38**, 240 (1983).

¹⁰M. Olivier, J. O. Strom-Olsen, Z. Altounian, and G. Williams, *J. Appl. Phys.* **53**, 769 (1982); J. A. Geohegan and S. M. Bhagat, *J. Magn. Magn. Mater.* **25**, 71 (1981); M. A. Manheimer, S. M. Bhagat, and H. S. Chen, *J. Magn. Magn. Mater.* **38**, 147 (1983); P. Hargraves and R. A. Dunlap, *J. Magn. Magn. Mater.* **75**, 378 (1988); A. T. Aldred and J. S. Kouvel, *Physica B* **86-88**, 329 (1977); U. Güntzel and K. Westerholt, *Phys. Rev. B* **41**, 740 (1990).

¹¹I. Ikeda and Y. Ishikawa, *J. Phys. Soc. Jpn.* **49**, 950 (1980).

¹²A. Das and A. K. Majumdar, *Phys. Rev. B* **43**, 6042 (1991).

¹³A. Das and A. K. Majumdar, *J. Appl. Phys.* **70**, 6323 (1991).

¹⁴E. W. Stanley, in *Introduction to Phase Transitions and Critical Phenomena* (Clarendon, Oxford, 1971), p. 1.

¹⁵J. S. Kouvel and M. E. Fisher, *Phys. Rev.* **136**, A1626 (1964).

¹⁶See sample No. 2 of Ref. 1. Other reports [see, e.g., P. Gaunt, S. C. Ho, G. Williams, and R. W. Cochrane, *Phys. Rev. B* **23**, 251 (1981)] of measurements on this sample give $T_c = 249$ K, but essentially the same $\gamma(T_c)$.

¹⁷A. Arrott and J. E. Noakes, *Phys. Rev. Lett.* **19**, 786 (1967).

¹⁸R. Hasegawa, *J. Appl. Phys.* **41**, 4096 (1970).

¹⁹S. N. Kaul, *Phys. Rev. B* **23**, 1205 (1981).

²⁰K. Yamada, Y. Ishikawa, Y. Endoh, and T. Masumoto, *Solid State Commun.* **16**, 1335 (1975).

²¹G. Aeppli, S. M. Shapiro, R. J. Birgeneau, and H. S. Chen, *Phys. Rev. B* **28**, 5161 (1983).

²²M. Seeger and H. Krönmüller, *J. Magn. Magn. Mater.* **28**, 393 (1989).

²³H.-O. Houer and D. Wagner, *Phys. Rev. B* **40**, 2502 (1989).